Available online at www.sciencedirect.com
ScienceDirect
Solid State Ionics 179 (2008) 1570–1574
SOLID STATE IONICS
www.elsevier.com/locate/ssi

Characteristics of ABO_3 and A_2BO_4 (A=Sm, Sr; B=Co, Fe, Ni) samarium oxide system as cathode materials for intermediate temperature-operating solid oxide fuel cell

Seung-Wook Baek, Jung Hyun Kim, Joongmyeon Bae *

Department of Mechanical Engineering, Korea Advanced Institute of Science and Technology, 373-1, Guseong-Dong, Yuseong-Gu, Daejeon, 305-701, Republic of Korea

Received 15 July 2007; received in revised form 23 November 2007; accepted 5 December 2007

Abstract

Samarium strontium cobalt oxide with ABO_3 lattice structure, which is mixed ionic and electronic conductor (MIEC), is considered as a promising cathode material for intermediate temperature-operating solid oxide fuel cell (IT-SOFC) due to its high electrocatalytic property. Cathode material containing cobalt (Co) is unstable at high temperature and has a relatively high thermal expansion coefficient. In this study, samarium oxide cathodes with ABO_3 and A_2BO_4 (A=Sm, Sr; B=Co, Fe, Ni) structure on $Sm_{0.2}Ce_{0.8}O_{1.9}$ electrolyte were investigated in terms of electrochemical property and thermal expansion property. Area specific resistance (ASR) was measured by ac impedance spectroscopy, and thermal expansion coefficient (TEC) was measured using a dilatometer. Microstructure of cathode was observed using a scanning electron microscopy. $Sm_{0.5}Sr_{0.5}CoO_{3-\delta}$ with ABO_3 structure showed the ASR of 0.87 Ωcm^2 at 600 °C, and $Sm_{0.5}Sr_{0.5}NiO_{3\pm\delta}$, which actually has A_2BO_4 structure, showed the lowest TEC value of 13.3×10^{-6}/K.

Keywords: ABO_3; A_2BO_4; Cathode; Solid oxide fuel cell

1. Introduction

In structural approach for SOFC cathode, spinel-structured (A_2BO_4) material has been suggested as another candidate of the cathode material for solid oxide fuel cell (SOFC) as spinel-structured oxides have relatively lower thermal expansion coefficient than that of perovskite structure [1–4]. Among several cathode materials, samarium oxide has recently been recognized as a promising cathode material for intermediate temperature-operating SOFC (IT-SOFC) due to its high electrocatalytic properties. Fukunaga et al. suggested the reaction model and reaction mechanism of $Sm_{0.5}Sr_{0.5}CoO_{3-\delta}$ cathode [5,6]. Performance of cell with $Sm_{0.5}Sr_{0.5}CoO_{3-\delta}$ and its composite cathode were reported by C. Xia et al. and X. Zhang et al., etc [7,8]. The aim of this work was to evaluate the electrochemical and thermal properties of the perovskite-structured and spinel-structured Sm-based oxides, and to discuss the feasibility of spinel-structured Sm oxide for application to IT-SOFC. Several transition metals were doped to the perovskite-structured $Sm_{0.5}Sr_{0.5}CoO_{3-\delta}$ and spinel-structured $Sm_{0.5}Sr_{1.5}CoO_{4\pm\delta}$ to improve the performance of cathode. Then, characteristics of $A_{0.5}A'_{0.5}B_xB'_{1-x}O_{3-\delta}$ (ABO_3) and $A_{0.5}A'_{1.5}B_xB'_{1-x}O_{4\pm\delta}$ (A_2BO_4) cathode materials (A=Sm, A′–Sr, B–Co, B′=Fe, Ni) on 20% Sm-doped cerium oxide ($Sm_{0.2}Ce_{0.8}O_{1.9}$, SDC) electrolyte were investigated.

2. Experimental

Cathode powders, synthesized by glycine nitrate process (GNP), were calcined for 1 h at 1250 °C. Crystal structures of synthesized powders were verified using an X-ray diffractometer (XRD, Rigaku). $Sm_{0.2}Ce_{0.8}O_{1.9}$ (SDC, Praxair) was

* Corresponding author. Tel.: +82 42 869 3045; fax: +82 42 869 8207.
E-mail address: jmbae@kaist.ac.kr (J. Bae).

0167-2738/$ - see front matter © 2007 Elsevier B.V. All rights reserved.
doi:10.1016/j.ssi.2007.12.010

used as an electrolyte material. Cathode materials were screen-printed on SDC electrolyte pellet, which is 1 mm in thickness, and sintered for 1 h at 1200 °C in air. SDC electrolyte pellet was made by uni-axial mold pressing with $50kg_f/cm^2$ and sintered for 4 h at 1500 °C. Electrochemical ac impedance measurements were conducted over temperature range of 450 °C to 900 °C in air. Specimens were measured by two electrode four probe method. Impedance spectra were measured by Solartron 1287/Solartron 1260 (electrochemical interface/impedance, gain-phase analyzer). Measuring frequency was from 5 MHz to 100 mHz, and ac amplitude of 50 mV was used for measurements. Thermal expansion coefficients (TEC) were measured by a dilatometer (TMA, Linseis) over range of 25 °C~900 °C to confirm the TEC compatibility of cell components.

3. Results

3.1. XRD patterns

Fig. 1 shows the XRD patterns of synthesized cathode materials. Rare earth element (Sr) is occupied on A-site of ABO_3 (perovskite structure) and A_2BO_4 (spinel structure), and transition metals are positioned on B-site. Fig. 1 (a) and (b) show the typical peaks of perovskite structure and spinel structure, respectively.

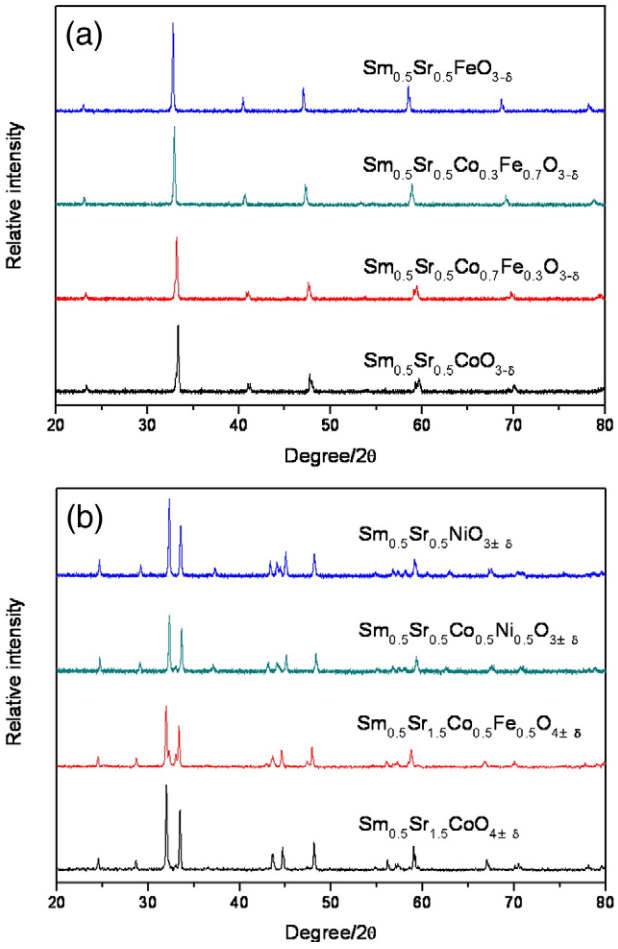

Fig. 1. XRD patterns of cathode materials. (a) ABO_3-structured Sm oxides, (b) A_2BO_4-structured Sm oxides.

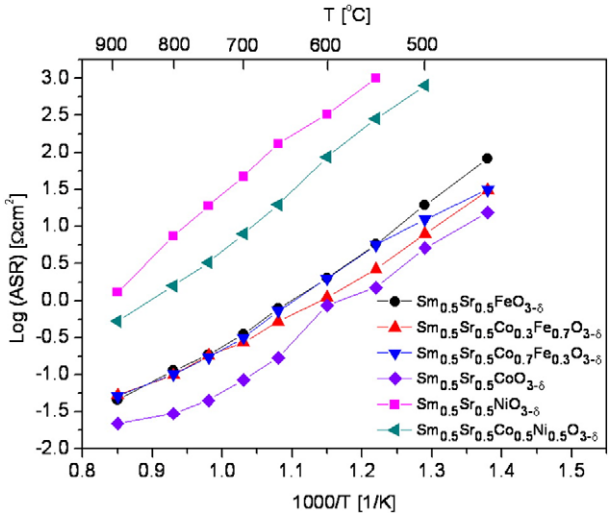

Fig. 2. ASR according to the substitution of B-site on $Sm_{0.5}Sr_{0.5}(Co, Fe, Ni)O_{3-\delta}$.

3.2. Area specific resistance (ASR)

Fig. 2 shows the plot of area specific resistance (ASR) at different temperatures when Fe and Ni were partially or wholly substituted on B-site of $Sm_{0.5}Sr_{0.5}CoO_{3-\delta}$ with ABO_3 structure. $Sm_{0.5}Sr_{0.5}CoO_{3-\delta}$ showed the best performance of 0.87 Ω cm^2 at 600 °C. Fig. 3 shows the ASR according to the partial substitution of B-site on $Sm_{0.5}Sr_{1.5}CoO_{4\pm\delta}$ with A_2BO_4 structure, and also shows the effect of sintering temperature for cathodic performance. ASR represents the overall cathodic properties related to the oxygen reduction, oxygen surface/bulk

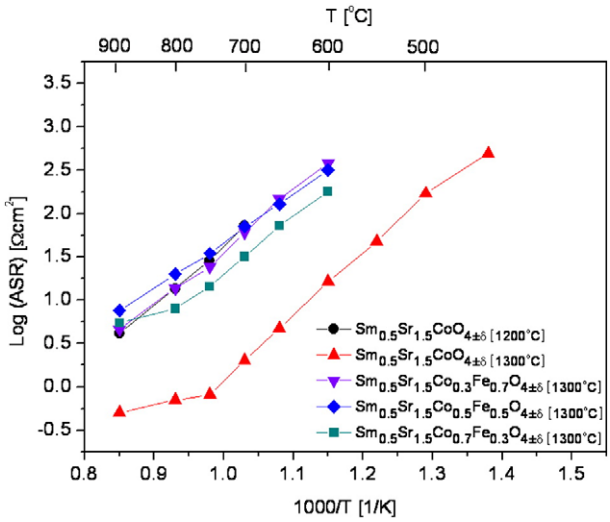

Fig. 3. ASR according to the substitution of B-site and sintering temperature of $Sm_{0.5}Sr_{1.5}(Co, Fe)O_{4\pm\delta}$.

Table 1
Material characteristics of the selected cathodes

Materials		E_a [eV]	ASR [Ωcm^2]	TEC[$\times 10^{-6}$/K]		
			600 °C	400 °C	600 °C	800 °C
Electrolyte	$Sm_{0.2}Ce_{0.8}O_{1.9}$	–	–	11.7	11.9	12.3
Perovskite	$Sm_{0.5}Sr_{0.5}CoO_{3-\delta}$	1.16	0.87	14.7	19.6	22.3
	$Sm_{0.5}Sr_{0.5}Co_{0.7}Fe_{0.3}O_{3-\delta}$	1.12	1.98	17.6	20.4	23.3
	$Sm_{0.5}Sr_{0.5}Co_{0.3}Fe_{0.7}O_{3-\delta}$	1.06	1.11	13.9	17.6	20.3
	$Sm_{0.5}Sr_{0.5}FeO_{3-\delta}$	1.24	2.00	12.3	16.0	18.3
Spinel	$Sm_{0.5}Sr_{0.5}Co_{0.5}Ni_{0.5}O_{3\pm\delta}$	1.49	87.50	15.4	15.6	15.8
	$Sm_{0.5}Sr_{0.5}NiO_{3\pm\delta}$	1.53	325	13.3	13.3	13.2
	$Sm_{0.5}Sr_{1.5}CoO_{4\pm\delta}$ [1300 °C]	1.23	16.37	20.2	19.7	20.0
	$Sm_{0.5}Sr_{1.5}Co_{0.7}Fe_{0.3}O_{4\pm\delta}$ [1300 °C]	1.06	180	6.4	10.2	13.0
	$Sm_{0.5}Sr_{1.5}Co_{0.5}Fe_{0.5}O_{4\pm\delta}$ [1300 °C]	1.08	317	10.5	19.8	20.3
	$Sm_{0.5}Sr_{1.5}Co_{0.3}Fe_{0.7}O_{4\pm\delta}$ [1300 °C]	1.29	380	15.8	16.3	17.0

diffusion and the gas-phase oxygen diffusion, and is defined as follow:

$$\mathrm{ASR} = \frac{\text{Resistance of electrode}}{2(\text{symmetry})} \times \text{Area of electrode}$$

3.3. Thermal expansion coefficient (TEC)

Thermal expansion coefficients (TEC) of ABO_3 and A_2BO_4-structured cathode materials are shown in Table 1. Fe substitution on B-site of ABO_3 and A_2BO_4 reduced TEC. However, TEC of Fe-substituted material was still larger than that of $Sm_{0.2}Ce_{0.8}O_{1.9}$ electrolyte at 600 °C. $Sm_{0.5}Sr_{0.5}Co_{0.5}Ni_{0.5}O_{3\pm\delta}$ and $Sm_{0.5}Sr_{0.5}NiO_{3\pm\delta}$ containing Ni showed the TEC values of 15.6×10^{-6}/K and 13.3×10^{-6}/K at 600 °C, respectively; however, remarkably increased ASR as shown in Fig. 2.

3.4. Microstructure

Fig. 4 shows the microstructure around the interface between $Sm_{0.5}Sr_{1.5}CoO_{4\pm\delta[1300\,°C]}$ cathode and $Sm_{0.2}Ce_{0.8}O_{1.9}$ electrolyte. The image was captured after $Sm_{0.5}Sr_{1.5}Co_{0.7}Fe_{0.3}O_{4\pm\delta[1300\,°C]}$ cathode was sintered at 1300 °C and ASR measured by impedance spectroscopy at 600 °C.

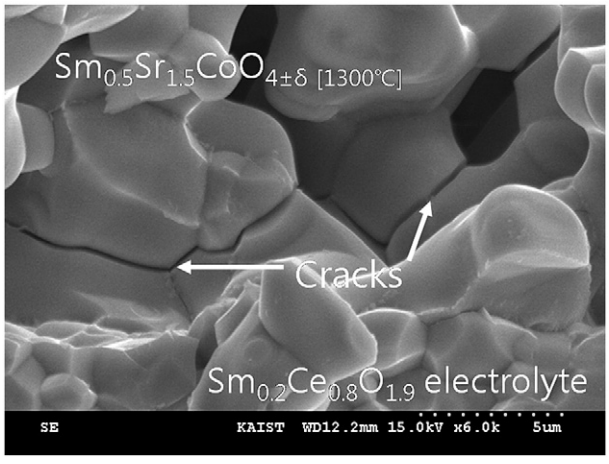

Fig. 4. Cracks at interface between $Sm_{0.5}Sr_{1.5}CoO_{4\pm\delta[1300\,°C]}$ cathode and $Sm_{0.2}Ce_{0.8}O_{1.9}$ electrolyte.

3.5. Impedance spectra

Figs. 5 and 6 show the impedance spectra of ABO_3-structured $Sm_{0.5}Sr_{0.5}CoO_{3-\delta}$ and A_2BO_4-structured $Sm_{0.5}Sr_{1.5}CoO_{4\pm\delta[1300\,°C]}$ at different temperature. Complex impedance response was separated to the individual responses of grain and grain boundary in the electrolyte, and electrode. R_g and R_{gb} represent the resistance by grain and grain boundary in the electrolyte, respectively. R_{ohmic} and $R_{electrode}$ mean the resistance by ohmic loss and the resistance of the electrode.

4. Discussion

Small peak shifts by substitution of elements were found using XRD. The phenomena are known due to the radius difference of substituted ions on lattice site. The ionic radius of Sm^{3+} on A-site is 0.096 nm and that of substituted Sr^{2+} is 0.144 nm. The ionic radius of Co^{3+} on B-site is 0.055 nm and

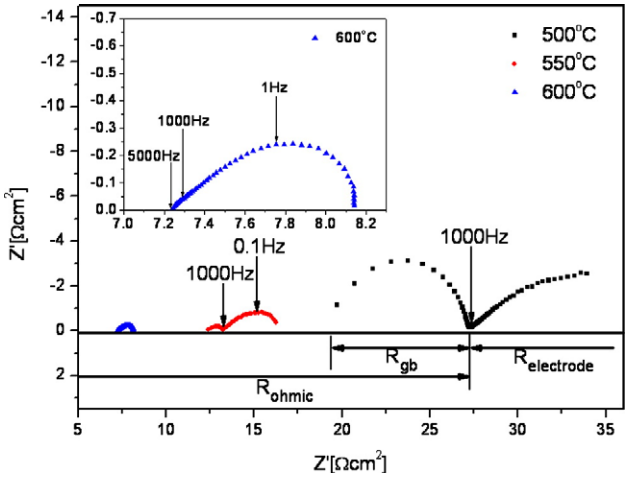

Fig. 5. Impedance spectra of $Sm_{0.5}Sr_{0.5}CoO_{3-\delta}$ cathode (R_{ohmic}: ohmic resistance, R_{gb}: resistance by electrolyte grain boundary, $R_{electrode}$: resistance of electrode).

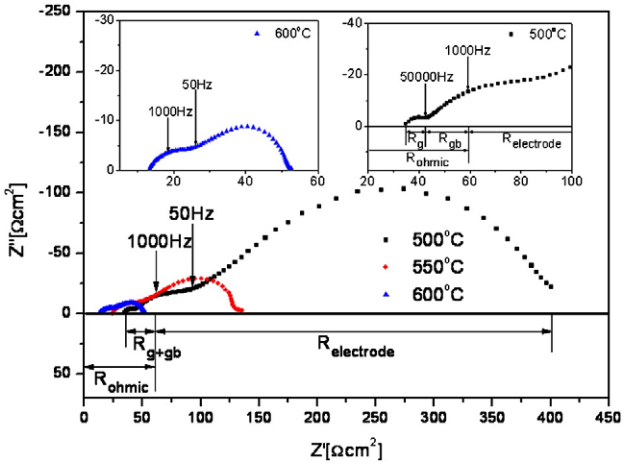

Fig. 6. Impedance spectra of $Sm_{0.5}Sr_{1.5}CoO_{4\pm\delta}$ cathode (R_{ohmic}: ohmic resistance, R_g: resistance by electrolyte grain, R_{gb}: resistance by electrolyte grain boundary, R_{g+gb}: resistance by electrolyte grain and grain boundary, $R_{electrode}$: resistance of electrode).

substituted Fe^{2+}, Fe^{3+} and Ni^{2+} are 0.078 nm, 0.065 nm and 0.069 nm, respectively [9,10]. Unit cell is expanded or contracted from ideal cubic structure by ionic radius difference and empty space of lattice, and also distorted [11,12]. Tolerance factor is introduced to measure the deviation from ideal unit cell [13]. Sm–Sr–(Co,Ni)–O system, containing abundant Ni, did not form perovskite structure, and changed to spinel structure as shown in Fig. 1. Formation of spinel structure is explained as electrovalence condition according to the substitution of A-site and the oxidation state of cations on B-site [3]. Charge neutrality is out of balance when Sr^{2+} is highly substituted on Sm^{3+} site. Disproportion of charge increases if Ni of +2 valence is highly doped on B-site instead of Co (mainly +3 valence). ABO_3 structure with cubic shape is not formed as the imbalance of lattice space is occurred by charge neutrality, and the amount of released oxygen increases.

In this research, substitution of Ni enhanced thermal expansion property of cathode. Favorable thermal expansion property is obtained without distortion or transformation of lattice minimizing absorption or release of oxygen ion when the small amount of Ni, about 0.1 mole, is doped. However, electrocatalytic property of $Sm_{0.5}Sr_{0.5}NiO_{3\pm\delta}$ was not satisfactory with high ASR values as seen in Fig. 2 although it showed the relatively low thermal expansion coefficient of 13.3×10^{-6}/K at 600 °C. $Sm_{0.5}Sr_{0.5}CoO_{3-\delta}$ of ABO_3 structure showed the best electrochemical performance of ASR 0.87 Ω/cm² at 600 °C. Activation energy of $Sm_{0.5}Sr_{0.5}Co_{0.3}Fe_{0.7}O_{3-\delta}$ was lowered from 1.16 eV of $Sm_{0.5}Sr_{0.5}CoO_{3-\delta}$ to 1.06 eV as Fe was substituted on B-site as shown in Table 1. However, electrocatalytic property was not acceptable and TEC was still higher than that of $Sm_{0.2}Ce_{0.8}O_{1.9}$ electrolyte (TEC of $Sm_{0.2}Ce_{0.8}O_{1.9}$ is 11.9×10^{-6}/K at 600 °C). $Sm_{0.5}Sr_{1.5}(Co,Fe)O_{4\pm\delta}$ series with A_2BO_4 structure showed a poor electrochemical cathode property and a little low TEC compared with $Sm_{0.5}Sr_{0.5}CoO_{3-\delta}$. A_2BO_4-structured cathode systems are thermodynamically stable and have higher oxidation state of B-site compared with ABO_3-structured cathode systems [1]. Nonetheless, sintering characteristic of A_2BO_4-structured $Sm_{0.5}Sr_{1.5}CoO_{4\pm\delta[1200\ °C]}$, such as adhesion property, was poor at 1200 °C. ASR became lowered when sintering temperature of $Sm_{0.5}Sr_{1.5}CoO_{4\pm\delta}$ increased to 1300 °C as shown in Fig. 3. A lot of cracks at interface between $Sm_{0.5}Sr_{1.5}CoO_{4\pm\delta[1300\ °C]}$ and $Sm_{0.2}Ce_{0.8}O_{1.9}$ electrolyte were observed so that paths of ion and electron decreased, and adhesion property to electrolyte was deteriorated as shown in Fig. 4.

Fig. 5 shows the impedance spectra of $Sm_{0.5}Sr_{0.5}CoO_{3-\delta}$ at different temperatures. Two semicircles are clearly shown at 500 °C and 550 °C. The semicircle of high frequency region over 1000 Hz is described as the resistance of grain boundary (R_{gb}) in the electrolyte [14]. The semicircle at high frequency is evident at low temperature; however, it is negligible as the temperature increases. The resistance of electrode ($R_{electrode}$) is involved in several cathode reactions such as oxygen adsorption/desorption process, charge transfer process, surface/bulk diffusion process and gas-phase diffusion process. The detailed consideration of $R_{electrode}$ for $Sm_{0.5}Sr_{0.5}CoO_{3-\delta}$ will be discussed at further study. Impedance spectra of spinel-structured $Sm_{0.5}Sr_{1.5}CoO_{4\pm\delta[1300\ °C]}$ are shown in Fig. 6. Two semicircles that are represented as the resistances of grain (R_g) and grain boundary (R_{gb}) in electrolyte are evident at 500 °C. It is considered that there is a semicircle at the medium frequency between 1000 Hz and 50 Hz. This semicircle represents the resistance associated with the oxygen ion transfer at electrode/electrolyte interface [15]. The large resistance of $Sm_{0.5}Sr_{1.5}CoO_{4\pm\delta[1300\ °C]}$ at medium frequency (1000 Hz~50 Hz) was caused by poor adhesion and cracks between $Sm_{0.5}Sr_{1.5}CoO_{4\pm\delta[1300\ °C]}$ cathode and $Sm_{0.2}Ce_{0.8}O_{1.9}$ electrolyte as shown in Fig. 4.

5. Conclusions

ABO_3-structured Sm-based oxides showed the better electrochemical performance than A_2BO_4-structured oxides although A_2BO_4-structured materials showed lower thermal expansion coefficient (TEC). Moreover, cathode sintering temperature of A_2BO_4-structured oxide to obtain good electrochemical property and adhesion property to electrolyte was higher than ABO_3-structured oxide. ABO_3-structured $Sm_{0.5}Sr_{0.5}CoO_{3-\delta}$ showed the ASR of 0.87 Ωcm² at 600 °C. Fe-substituted cathodes on B-site of $Sm_{0.5}Sr_{0.5}CoO_{3-\delta}$ and $Sm_{0.5}Sr_{1.5}CoO_{4\pm\delta}$ didn't show the sufficiently enhanced ASR and TEC. For Sm-based oxides, it is considered that lowering TEC of Sm-based cathode materials with ABO_3 structure, using composite cathode, is more beneficial than using A_2BO_4-structured Sm oxides for operating SOFC below 600 °C.

Acknowledgment

This work is an outcome of the projects of the development program of Core Technologies for Fuel Cells (CTFC) and the Best Lab program of the Ministry of Commerce, Industry and Energy (MOCIE), and the Brain Korea 21 (BK21) program of the Ministry of Education and Human Resources Development (MOE) of Korea. The authors greatly appreciate the financial support from these organizations.

References

[1] M. Al Daroukh, V.V. Vashook, H. Ullmann, F. Tietz, I. Arual Raj, Solid State Ionics 158 (2003) 141.

[2] Y. Wang, H. Nie, S. Wang, T. Wen, U. Guth, V. Valshook, Materials Letters 60 (2006) 1174.

[3] H.W. Nie, T.L. Wen, S.R. Wang, Y.S. Wang, U. Guth, V. Vashook, Solid State Ionics 177 (2006) 1929.

[4] A. Aguadero, M.J. Escudero, M. Pérez, J.A. Alonso, L. Daza, Transactions of the American Society of Mechanical Engineers 4 (2007) 294.

[5] H. Fukunaga, M. Koyama, N. Takahashi, C. Wen, K. Yamada, Solid State Ionics 132 (2000) 279.

[6] M. Koyama, C. Wen, T. Masuyama, J. Otomo, H. Fukunaga, K. Yamada, K. Eguchi, H. Takahashi, Journal of the Electrochemical Society 148 (7) (2001) A795.

[7] C. Xia, W. Rauch, F. Chen, M. Liu, Solid State Ionics 149 (2002) 11.

[8] X. Zhang, M. Robertson, S. Yick, C. Deĉes-Petit, E. Styles, W. Qu, Y. Xie, R. Hui, J. Roller, O. Kesler, R. Maric, D. Ghosh, Journal of Power Sources 160 (2006) 1211.

[9] G.Ch. Kostogloudis, P. Fertis, Ch. Ftikos, Solid State Ionics 118 (1999) 241.

[10] Y.M. Chiang, D. Birnie, W.D. Kingery, Physical ceramics, John Wiley & Sons, Ltd., MIT, US, 1997.

[11] S.P. Simner, J.P. Shelton, M.D. Anderson, J.M. Stevenson, Solid State Ionics 161 (2003) 11.

[12] Masashi Mori, Solid State Ionics 174 (2004) 1.

[13] G.Ch. Kostoglouodis, N. Vasilakos, Ch. Ftikos, Journal of the European Ceramic Society 17 (1997) 1513.

[14] J. Bae, Ph.D. Thesis, Centre for Technical Ceramics, Imperial College, 1996.

[15] F.S. Baumann, J. Fleig, H. Habermeier, J. Maier, Solid State Ionics 177 (2006) 1071.